Coupled Systems Mechanics, *Vol. 11, No. 4 (2022) 335-355*
https://doi.org/10.12989/csm.2022.11.4.335

Free vibration analysis of steel liquid storage tank with functionally graded column based on modified continuum mechanics

Yakup Harun Çavuş*, Togay Küpeli[a] and Mustafa Özgür Yaylı[b]

Department of Civil Engineering, Faculty of Engineering, Bursa Uludag University, Bursa, Türkiye

(Received December 20, 2021, Revised April 25, 2022, Accepted May 15, 2022)

Abstract. It's important to note that the number of studies on the lateral vibration of steel liquid storage tanks has been quite modest in the past. The aim of this research has to look at the variables that affect vibration of storage tanks and to highlight the characteristics of a construction that hasn't received much attention in the literature. The storage tank has pre-sized in the study, and aluminum and steel have chosen as components. The specified material qualities and the factors utilized in the investigation has used to calculate vibration frequency values. The resulting calculations are backed up by tables and graphs, and it's an important to look into the parameters that affect the vibration frequencies that will occur on the designed storage tank vary. In the literature, water tanks are usually modelled as lumped masses. The horizontal stiffness of the column on which it is placed is assumed to be constant throughout. This is an approximation method of solving this problem. The column is handled in this study with a more realistic approach that fits the continuum mechanics in the analysis. The reservoir part is incorporated directly into the problem as the boundary condition.

Keywords: Fourier series; functionally graded materials; nonlocal elasticity theory; steel liquid storage tanks; vibration analysis

1. Introduction

It is noteworthy that among the studies have conducted in the past, the number of those on the lateral vibration of steel liquid storage tanks is limited. Most of the existing studies are related to rectangular liquid storage tanks or the design of these tanks. There are many different methods in seismic design of storage tanks and the most common of these is the Housner method. Two of the most important design standards are Eurocode 8 and ACI 350. There are many studies in the literature with this design method and standards. In terms of geometric shape, most of the previous studies are related to rectangular liquid storage tanks.

The reasons why liquid storage tanks are made of steel are that they are stainless, galvanized,

*Corresponding author, Ph.D. Student, E-mail: yakupharuncavus@gmail.com
[a]Ph.D. Student, E-mail: togay-kupeli@hotmail.com
[b]Associate Professor, E-mail: ozguryayli@uludag.edu.tr

http://www.techno-press.org/?journal=csm&subpage=8 ISSN: 2234-2184 (Print), 2234-2192 (Online)

economical, have high durability and do not produce odor. Although high thermal conductivity is a disadvantage for storage, this disadvantage can be avoided by providing internal insulation. Likewise, the high coefficients of thermal expansion of steels are also a disadvantage for their use for storage purposes and these properties of steels should be taken into account at the design stage.

Kotrasova *et al*. have studied about dynamic analysis of liquid storage tanks. Theoretical background of seismic reaction liquid storage circular container has been discussed in extensively in this work. Chen *et al*. have analyzed for seismic analysis for SDOF system rectangular liquid storage tanks which made of concrete. The subject of seismic analysis and design of concrete rectangular liquid storage tanks has been thoroughly investigated utilizing a simplified method based on the generalized single degree of freedom (SDOF) method. Ruiz *et al*. have worked on an efficient computational method for dynamic analysis of liquid storage tanks. The study has been the subject of several reports about numerical model for analyzing the dynamic behavior of liquid storage tanks which is computationally efficient. Nam Phan *et al*. have analyzed seismic fragility of steel storage tanks which supported by reinforced concrete columns. The paper has submitted the seismic susceptibility of elevated steel storage tanks supported by reinforced concrete columns using a probabilistic seismic assessment approach. Veletsos has investigated the effects of the earthquake on flexible liquid storage tanks. Ali *et al*. have compared the dynamic analysis of cylindrical liquid storage tanks according to EUROCODE 8 and ACI350. The engineers who have to calculate liquid tanks according to earthquakes or who are interested in this subject will benefit from the study's content, which will help them understand the behavior of liquid tanks under dynamic loads, compare the regulations for these, and contribute to the calculation and design of liquid tank has determined as the main subject of the work. Chen *et al*. have studied about dynamic analysis of rectangular liquid storage tanks which made of concrete. The model used in the paper encompasses the influence of tank wall flexibility on hydrodynamic pressures and employs the consistent mass approach effect. Haroun has written a thesis about dynamic analysis of liquid storage tanks.

Vukobratovic *et al*. have analyzed seismic analysis of circular liquid storage tanks. The findings of a simplified analysis of the total seismic response of ground-supported concrete circular liquid storage tanks with varying geometrical features are provided in this article. Kozluca *et al*. have studied for economical design of concrete cylindrical liquid storage tanks. The most cost-effective warehouse radius-tank height ratio and designs have been created by varying the and radius values in this paper. Haroun *et al*. have investigated the effects of the earthquake on the deformable liquid storage tanks. Larkin has researched relations between soil and structure seismic behavior of under the effects of the earthquake. Chen has written a thesis about dynamic analysis of concrete rectangular liquid storage tanks. Malhotra *et al*. have improved a method for seismic analysis of liquid storage tanks. In flexible steel or concrete tanks fixed to rigid foundations, the technique takes into consideration the liquid's impulsive and convective (sloshing) motions. The main factors are calculating seismic responses, base shear, overturning force, and sloshing wave height, utilizing the site response spectra and completing a few simple calculations. Dogangun has written a thesis about seismic analysis of rectangular liquid storage tanks considering the relation between soil, liquid and storage tank using finite elements method. Sabuncu *et al*. have analyzed seismic vibration of liquid storage tanks. The period and damping ratio of the structure has determined from the vibration recordings, according to the study's content. In addition, a solution has found by modeling the water tank structural analysis programs in compliance with the project. The dynamic properties derived from the vibration records has compared to the analysis results obtained from the project data.

Kasimzade *et al*. have published a paper about obtaining dynamic parameters by using ambient vibration recordings on model of the steel arch bridge. This study presents the dynamic parameters acquired from the operational modal analysis of the model steel arch bridge has compared to the analytical parameters derived from the model steel arch bridge using the finite element approach. The topic of the effect of continuous suspension constraint on the free vibration and buckling of a beam has been covered by Németh *et al*. A continuously suspending simply-supported beam's free vibration and buckling are investigated in this paper. Györgyi has conducted the subject of frequency-dependent geometrical stiffness matrix for the vibration analysis of beam systems. The question of frequency-dependent geometrical stiffness matrices of beams has been inferred by taking shear deformations has been addressed in this paper. The article titled random structural dynamic response analysis under random excitation have shared by Jun *et al*. The mean and covariance matrix of the random response of stochastic structures characterized by FE models are computed using a numerical approach has been covered in this research article. The nonlocal strain gradient theory is used in the context of nonclassical continuum mechanics to develop a nonclassical size dependent model to investigate the dynamic behavior of a CNTs reinforced composite beam resting on two parameters elastic foundations under a moving load. Similar studies on this subject have been published. Abdelrahman *et al*. have investigating dynamic analysis of FG nanobeam reinforced by carbon nanotubes and resting on elastic foundation under moving load. Esen *et al*. have published an article about on vibration of sigmoid/symmetric functionally graded nonlocal strain gradient nanobeams under moving load. Free vibration of porous FG nonlocal modified couple nanobeams via a modified porosity model have indicated by Ghandourah *et al*. Dynamics of perforated higher order nanobeams subject to moving load using the nonlocal strain gradient theory has studied by Abdelrahman *et al*. Dynamic analysis of structures supporting a moving mass, exposed to external and internal damping has published by Györgyi. This study presents a method for analyzing dynamic excess displacements of buildings in circumstances where both the impacts of moving mass and internal friction must be considered.

There are several works on vibration analysis of nanostructures in the literature. Dynamic instability behavior of functionally graded carbon nanotube reinforced hybrid composite plates subjected to periodic loadings have studied by Chen *et al*. Beni *et al*. have investigated the nonlinear forced vibration of isotropic viscoelastic/piezoelectric Euler-Bernoulli nano-beam. The vibration and buckling of a double-layer Graphene sheet (DLGS) coupled with a piezoelectric nanoplate through an elastic medium (Pasternak and Winkler models) have conducted by Fard *et al*. One of the other vibration analyses of axisymmetric vibration of functionally-graded circular nano-plate based on the integral form of the strain gradient model has examined by Pourabdy *et al*., in this study they aimed to analyze the linear vibrational behavior of functionally-graded (FG) size-dependent circular nano-plates using the integral form of the non-local strain gradient (NSG) model. Soliman *et al*. have published study on nonlinear transient analysis of FG pipe subjected to internal pressure and unsteady temperature in a natural gas facility. The response of functionally graded (FG) gas pipe under unsteady internal pressure and temperature is investigated in that study. An original hyperbolic and parabolic shear and normal deformation theory for the bending analysis to account for the effect of thickness stretching in functionally graded (FG) sandwich plates indicated by Daouadji *et al*. The vibration of an electrostatically actuated micro cantilever beam analyzes have published by Poloei *et al*. Analysis of crack occurs under unsteady pressure and temperature in a natural gas facility by applying FGM has investigated by Soliman *et al*. In this article Soliman and the others subjected to functionally graded material (FGM) is benefit from the ceramics durability and its surface hardness against erosion. Another study on free vibration

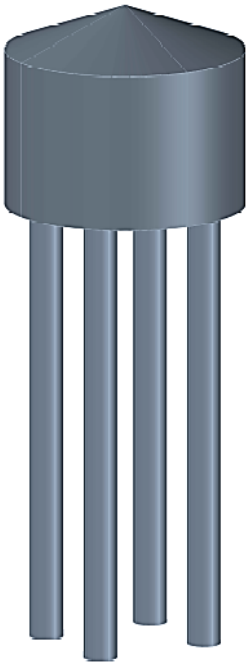

Fig. 1 A water tower made of steel material

analysis has presented by Rossit *et al*. The free transverse vibrations of axially functionally graded (AFG) cantilever beams with concentrated masses attached at different points has investigated in this study.

The materials utilized in this research have been steel-aluminum and zirconia (ZrO_2)-aluminum. The column is pre-sized according to the weak material in this pre-sizing (according to aluminum). To preserve the homogeneous material in the safe zone, r was determined as follows in this pre-sizing. Buckling analysis and pre-sizing have been accomplished because buckling will be prominent in the 40m column. Vibration frequency analyses on various parameters have been carried out once the design phase of the water tank has been completed.

These parameters, as well as the values of the selected materials, have been subjected to vibration frequency analysis. Graphs and tables have been used to present the findings. It has attempted to demonstrate how parameter values effect vibration frequency by changing parameter values. The calculations within the scope of this study were made on the idealized model (Fig. 2) of the water tower (Fig. 1). In the model, a spring is used to manage the vibration frequencies and amplitudes. To design the amplitude and frequency appropriately, the compression coefficient of the spring can be as large or as small as preferred.

2. Formulations

A variety of beam theories are utilized to represent the kinematics of deformation. We present the following coordinate system to define the various beam theories. The x-coordinate is measured along the length of the beam, the z-coordinate is measured along the thickness (height) of the

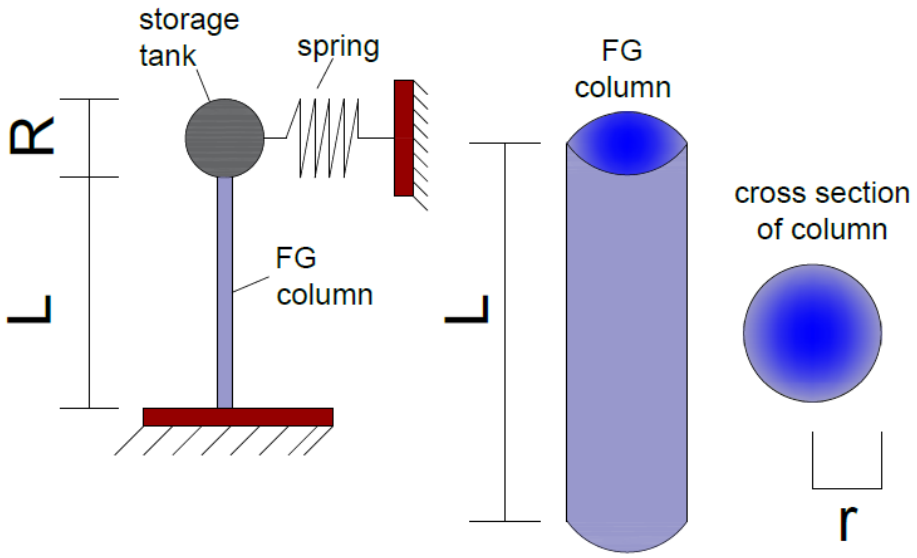

Fig. 2 Idealized model of water tower

beam, and the y-coordinate is determined along the width of the beam. All applied loads and geometry in a beam theory are such that displacements (u_1, u_2, u_3) along the coordinates (x, y, z) are solely functions of the x and z coordinates and time t. It is also assumed that the displacement u_2 is identically zero in this case. The following stress outcomes are introduced for use in the following sections

$$N = \int_A \sigma_{xx} dA, \quad M = \int_A z\sigma_{xx} dA \tag{1}$$

Euler Beam Theory (EBT), which is based on the displacement field

$$u_1 = u(x,t) - z\frac{\partial w^E}{\partial x}, \quad u_2 = 0, \quad u_3 = w^E(x,t) \tag{2}$$

where (u, w^E) expresses the longitudinal and transverse displacements of the point $(x, 0)$ on the beam's mid-plane (**i. e.**, $z = 0$) and the superscript 'E' represents the constants in the Euler-Bernoulli beam theory.

$$\varepsilon_{xx}^E = \frac{\partial u}{\partial x} - z\frac{\partial^2 w^E}{\partial x^2} \equiv \varepsilon_{xx}^0 + z\kappa^E, \quad \varepsilon_{xx}^0 = \frac{\partial u}{\partial x}, \quad \kappa^E = -\frac{\partial^2 w^E}{\partial x^2} \tag{3}$$

where ε_{xx}^0 represents the extensional strain and κ^E denotes the bending strain. The virtual displacements approach has the following form

$$\begin{aligned} 0 = \int_0^T \int_0^L [m_0(\frac{\partial u}{\partial t}\frac{\partial \delta u}{\partial t} + \frac{\partial w^E}{\partial t}\frac{\partial \delta w^E}{\partial t}) + m_2 \frac{\partial^2 w^E}{\partial x \partial t}\frac{\partial^2 \delta w^E}{\partial x \partial t} - N\delta\varepsilon_{xx}^0 - M^E\delta\kappa^E \\ + f\delta u + q\delta w^E + \overline{N}^E \frac{\partial w^E}{\partial x}\frac{\partial \delta w^E}{\partial x}]dxdt \end{aligned} \tag{4}$$

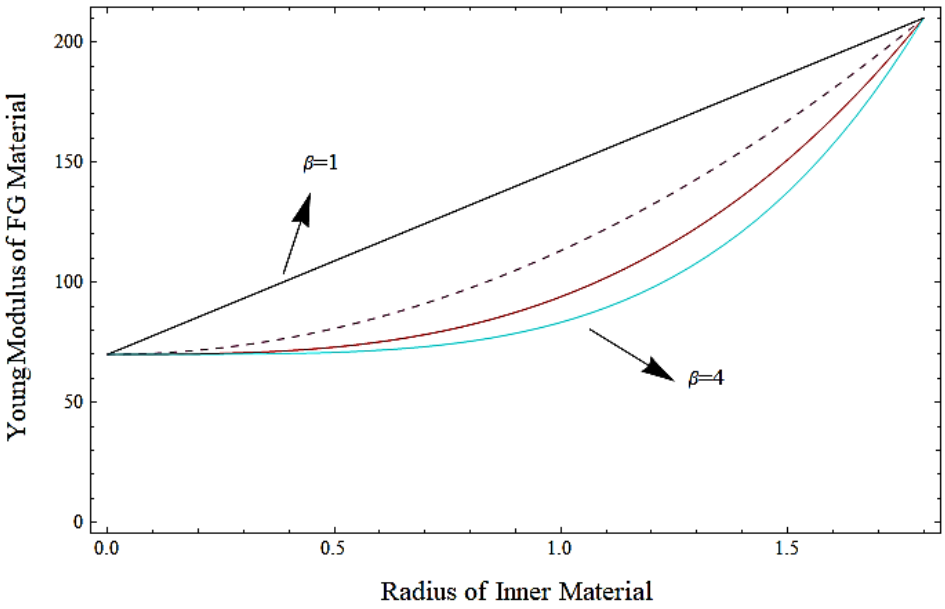

Fig. 3 Young Modulus (GPa) of FG Material (steel-aluminum) values related to different FG index values

$f(x, t)$ and $q(x, t)$ are the axial and transverse distributed forces (measured for each unit length), respectively, and $\overline{N}^E$ is the applied axial compressive force. In $0<x<L$, we get the following Euler-Lagrange equations.

$$\frac{\partial N}{\partial x} + f = m_0 \frac{\partial^2 u}{\partial t^2} \tag{5}$$

$$\frac{\partial^2 M^E}{\partial x^2} + q - \frac{\partial}{\partial x}\left(\overline{N}^E \frac{\partial w^E}{\partial x}\right) = m_0 \frac{\partial^2 w^E}{\partial t^2} - m_2 \frac{\partial^4 w^E}{\partial x^2 \partial t^2} \tag{6}$$

The boundary conditions encompass specifying one element from each of the three pairs among $x=0$ and $x=L$

$$\begin{aligned} & u \quad \text{or} \quad N \\ & w^E \quad \text{or} \quad \frac{\partial M^E}{\partial x} - \overline{N}^E \frac{\partial w^E}{\partial x} + m_2 \frac{\partial^3 w^E}{\partial x \partial t^2} \equiv V^E \\ & -\frac{\partial w^E}{\partial x} \quad \text{or} \quad M^E \end{aligned} \tag{7}$$

The equivalent shear force is represented by V^E in this particular instance. By using the nonlocal elasticity theory, the fourth-order partial differential equation of a column was found by Reddy in 2007 as follows.

$$E_{FGM} I \frac{\partial^4 v(x,t)}{\partial x^4} + \rho_{FGM} A \frac{\partial^2 v(x,t)}{\partial t^2} = 0 \tag{8}$$

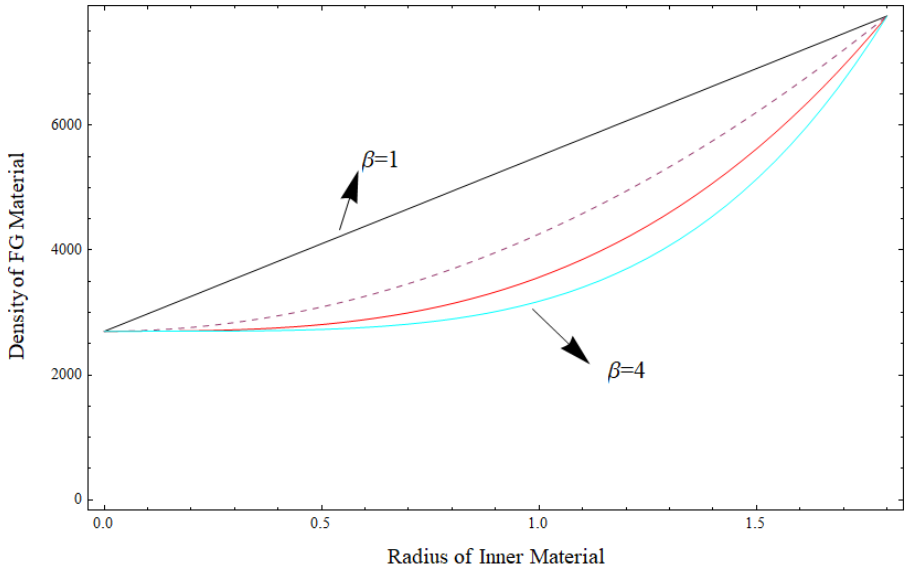

Fig. 4 Density (kg/m^3) of FG Material (steel-aluminum) values related to different FG index values

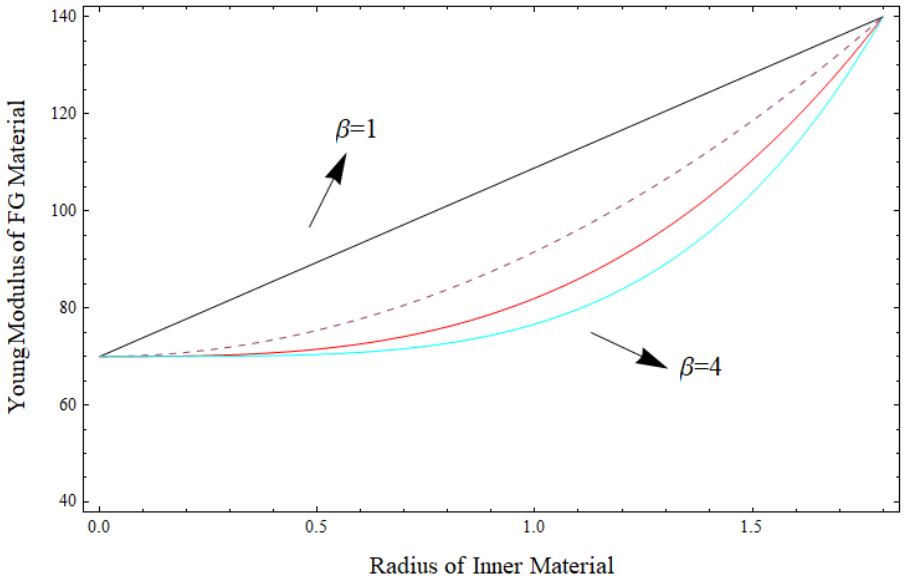

Fig. 5 Young Modulus (GPa) of FG Material (zirconia-aluminum) values related to different FG index values

where E_{FGM} is the flexural rigidity of functional graded material of column, E is the Young's modulus, I is the moment of inertia of the cross-sectional area A, ρ_{FGM} is the density of the functional graded material of column.

$$E_{FGM} = ((E_o - E_i)(\frac{r}{R})^{\beta} + E_i) \tag{9}$$

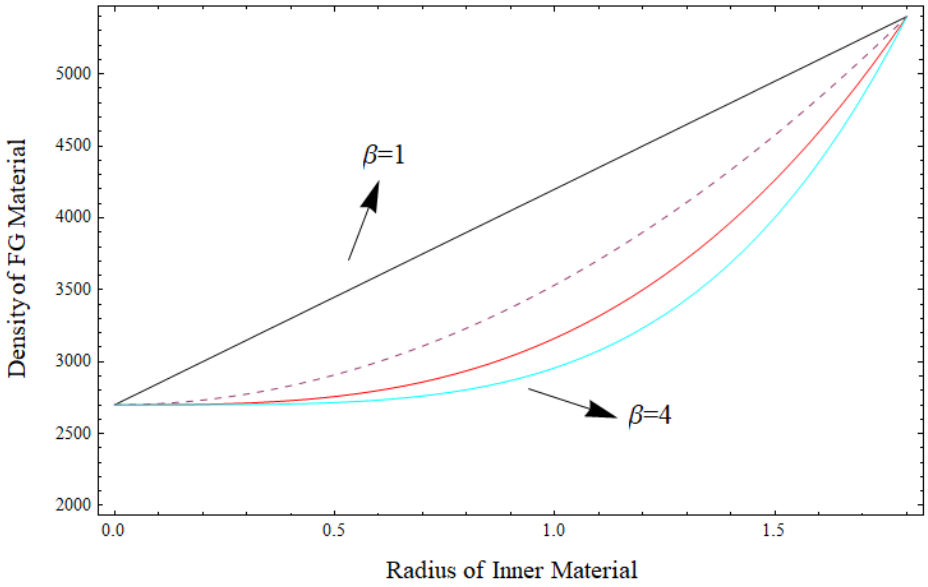

Fig. 6 Density (kg/m^3) of FG Material (zirconia-aluminum) values related to different FG index values

$$\rho_{FGM} = ((\rho_o - \rho_i)(\frac{r}{R})^{\beta} + \rho_i) \tag{10}$$

$$E_{FGM} I = \pi \int_0^R [(E_o - E_i)(\frac{r}{R})^{\beta} + E_i] r^3 dr \tag{11}$$

$$\rho_{FGM} A = 2\pi \int_0^R [(\rho_o - \rho_i)(\frac{r}{R})^{\beta} + \rho_i] r dr \tag{12}$$

In this case, the multiplying of the modulus of elasticity and the moment of inertia and the multiplying of ρ and the cross-sectional area can be expressed as above. The functionally graded material function given in Eqs. (11) and (12) has been used in many past studies. Although it is not the same as in this study, there are studies close to this formulation in the literatüre (Civalek 2021, 2022(a) and 2022(b)). In Figs. 3 and 4, respectively, the graphs of the elasticity modulus and density values of the functionally graded material are presented according to the grading function. $v(x,t)$ describes the lateral displacement used to describe the lateral vibration of the column.

$$v(x,t) = \Psi(x)\cos(\omega t) \tag{13}$$

In this equation, ω is the natural frequency and $\Psi(x)$ is the modal displacement function. After establishing the relations between the boundary points, the following modal displacement function emerges (Yayli 2015)

$$\Psi(x) = \begin{bmatrix} \Psi_0 & x = 0 \\ \Psi_L & x = L \\ \sum_{j=1}^{\infty} D_j \sin(\alpha_j x) & 0 < x < L \end{bmatrix} \tag{14}$$

In order to provide flexibility in boundary conditions, two different approximation functions are chosen separately in this study, within the region and in the boundary conditions. As it is known, Fourier sine series work for structures that simply supported beam. However, Fourier sine series will not work in boundary conditions except simple support. Since the Stokes transform, which is a mathematical transformation, is used in this study, the choice of sine or cosine is not important. Wherein

$$\alpha_j = \frac{j\pi}{L} \tag{15}$$

where L describes the column's length. This equation consists of an infinite series. However, in order to be able to calculate in a computer program, this infinite series must be truncated somewhere. More than one solution was made to determine where this truncation would take place, and the series was truncated where the solutions were almost equal to each other. The Fourier coefficient in Eq. (14), D_j, can be obtained as follows

$$D_j = \frac{2}{L}\int_0^L v(x)\sin(\alpha_j x)\partial x \tag{16}$$

Eq. (14) can be written as follows to provide the conditions

$$v'(x) = \sum_{k=1}^{\infty} \alpha_j D_j \cos(\alpha_j x) \tag{17}$$

Fourier cosine series can be defined as

$$v'(x) = \frac{r_o}{L} \sum_{j=1}^{\infty} r_j \cos(\alpha_j x) \tag{18}$$

The Fourier coefficients in Eq. (18) are obtained as follows

$$r_o = \frac{2}{L}\int_0^L v'(x)\partial x = \frac{2}{L}[v(L) - v(0)] \tag{19}$$

$$r_j = \frac{2}{L}\int_0^L v'(x)\cos(\alpha_j x)\partial x, (j = 1, 2...) \tag{20}$$

The following results are obtained when the partial integrals are calculated

$$r_j = \frac{2}{L}[v(x)\cos(\alpha_j x)] + \frac{2}{L}[\alpha_j \int_0^L v(x)\sin(\alpha_j x)]\partial x \tag{21}$$

$$r_j = \frac{2}{L}[(-1)^j v(L) - v(0)] + \alpha_j D_j \tag{22}$$

The first derivative of the function is as given below

$$\frac{\partial v(x)}{\partial x} = \frac{\psi_L - \psi_0}{L} + \sum_{j=1}^{\infty} \cos(\alpha_j x)(\frac{2((-1)^j \psi_L - \psi_0)}{L} + \alpha_j D_j) \tag{23}$$

The equations given above are a brief summary of the Stokes' transformation. Using the

following Stokes transform, higher order derivatives of $v(x)$ in Eq. (29) can be obtained separately.

$$\frac{\partial^2 v(x)}{\partial x^2} = -\sum_{j=1}^{\infty} \alpha_j \sin(\alpha_j x)\left(\frac{2((-1)^j \psi_L - \psi_0)}{L} + \alpha_j D_j\right) \tag{24}$$

$$\frac{\partial^3 v(x)}{\partial x^3} = \frac{\psi_L{}'' - \psi_0{}''}{L} + \sum_{j=1}^{\infty} \cos(\alpha_j x)\left(\frac{2((-1)^j \psi_L{}'' - \psi_0{}''}{L} - \alpha_j^2 \frac{2((-1)^j \psi_L - \psi_0)}{L} + \alpha_j D_j\right) \tag{25}$$

$$\frac{\partial^4 v(x)}{\partial x^4} = -\sum_{j=1}^{\infty} \alpha_j \sin(\alpha_j x)\left(\frac{2((-1)^j \psi_L{}'' - \psi_0{}'')}{L} - \alpha_j^2 \frac{2((-1)^j \psi_L - \psi_0)}{L} + \alpha_j D_j\right) \tag{26}$$

When Eqs. (24) and (26) are used instead of expressions in Eq. (8)

$$\sum_{j=1}^{\infty}\left(\frac{2}{L}\cos(\omega t)\sin(\alpha_j x)(-LD_j(\rho_{FGM} A\omega^2 - E_{FGM} I\alpha_j^4) - 2\alpha_j((-1)^j(\psi_L(-E_{FGM} I\alpha_j^2) + E_{FGM} I\psi_L{}''\right.$$
$$\left. + \psi_0(E_{FGM} I\alpha_j^2) + E_{FGM} I\psi_L{}'' = 0\right. \tag{27}$$

In Eq. (27), the Fourier coefficient is equal to the squareroot of the Eq. (27) can be written as follows in terms of ψ_0, ψ_L, $\psi_0{}''$ and $\psi_L{}''$

$$D_j = \frac{2(\omega^2)_j}{-(\omega^2)_j + \omega^2}((\psi_0{}'' - (-1)^j \psi_L{}'') - \alpha_j^2(\psi_0 - (-1)^j \psi_L)) \tag{28}$$

The free vibration of a column with free support at both ends is represented by the function $v(x,t)$.

$$v(x,t) = \sum_{j=1}^{\infty} \frac{2(\omega^2)_j}{-(\omega^2)_j + \omega^2}((\psi_0{}'' - (-1)^j \psi_L{}'') - \alpha_j^2(\psi_0 - (-1)^j \psi_L))\cos(\omega t)\sin(\alpha_j x) \tag{29}$$

This function is applicable to all boundary conditions and is a more general and applicable version of existing techniques.

3. Defined boundaries

It is accepted that the structure to be used in this study has a mass at the free end and a column with a fixed support at the other end. The boundary conditions just mentioned are expressed mathematically as

$$\psi_0 = 0, \quad \frac{\partial v(x,t)}{\partial x} = 0, \quad x = 0 \tag{30}$$

$$\psi_L{}'' = 0, k\psi_L - m\frac{\partial^2 v(x,t)}{\partial t^2} = E_{FGM} I \frac{\partial^3 v(x,t)}{\partial x^3}, x = L \tag{31}$$

Substituting the expressions obtained in Eqs. (23), (25) and (28) at the corresponding places in Eqs. (30) and (31) yields two simultaneous homogeneous equations.

$$(1+\sum_{j=1}^{\infty}\frac{2\lambda^4(-1)^j}{\lambda^4-j^4})\psi_L+(K-m\pi^2\lambda^4+\sum_{j=1}^{\infty}\frac{2\lambda^4(-1)^j}{\lambda^4-j^4})\psi_0{}''=0 \tag{32}$$

$$(\sum_{j=1}^{\infty}\frac{2j^2}{\pi^2(\lambda^4-j^4)})\psi_L+(1+\sum_{j=1}^{\infty}\frac{2\lambda^4(-1)^j}{\lambda^4-j^4})\psi_0{}''=0 \tag{33}$$

In which

$$\lambda^4=\frac{\rho_{FGM}AL^4\omega^2}{\pi^4E_{FGM}I} \tag{34}$$

$$K=\frac{kL^3}{E_{FGM}I} \tag{35}$$

Eqs. (32) and (33) can be represented in matrix form as

$$\begin{bmatrix}\phi_{11} & \phi_{12}\\ \phi_{21} & \phi_{22}\end{bmatrix}\begin{bmatrix}\psi_L\\ \psi_0{}''\end{bmatrix}=0 \tag{36}$$

Wherein

$$\phi_{11}=1+\sum_{j=1}^{\infty}\frac{2\lambda^4(-1)^j}{\lambda^4-j^4} \tag{37}$$

$$\phi_{12}=K-m\pi^4\lambda^4+\sum_{j=1}^{\infty}\frac{2\lambda^4\pi^2j^2}{\lambda^4-j^4} \tag{38}$$

$$\phi_{21}=\sum_{j=1}^{\infty}\frac{2j^2}{\pi^2(\lambda^4-j^4)} \tag{39}$$

$$\phi_{22}=1+\sum_{j=1}^{\infty}\frac{2\lambda^4(-1)^j}{\lambda^4-j^4} \tag{40}$$

The relation given in Eq. (36) is presented as the equation of an eigenvalue problem. If the determinant of the coefficient matrix presented in Eq. (34) is taken and this determinant equation is set to “0”, the mentioned eigenvalues can be easily obtained.

$$\begin{vmatrix}\phi_{11} & \phi_{12}\\ \phi_{21} & \phi_{22}\end{vmatrix}=0 \tag{41}$$

By using different (K) and (m) values to be used for different boundary conditions, the determinant given above can be used to solve different problems.

4. Consequences of vibration analysis

In this section, lateral vibration analyzes of a steel liquid storage tank designed as a water tower are presented within the scope of this study. The designed water tower model consists of three

Table 1 Mechanical properties of materials

	E (Young's modulus) GPa	ρ (Density) kg/m^3
Steel	210	7750
Zirconia	140	5400
Aluminum	70	2700

Table 2 Frequency parameter values (rad/s) for various FG (steel-aluminum) index values

	$\beta = 0$	$\beta = 1$	$\beta = 2$	$\beta = 3$	$\beta = 4$
Mode 1	10.0009	10.523	10.7417	10.8306	10.8578
Mode 2	28.8989	30.4377	31.0396	31.2966	31.3750
Mode 3	32.3745	34.0646	34.7726	35.0605	35.1483
Mode 4	40.8692	43.0029	43.8967	44.2601	44.3710
Mode 5	43.4381	45.7059	46.6559	47.0421	47.1600
Mode 6	50.0543	52.6676	53.7622	54.2073	56.6808

Table 3 Frequency parameter values (rad/s) for various FG (zirconia-aluminum) index values

	$\beta = 0$	$\beta = 1$	$\beta = 2$	$\beta = 3$	$\beta = 4$
Mode 1	9.7824	10.1662	10.3116	10.3640	10.3758
Mode 2	28.2676	29.3766	29.7967	29.8848	29.9824
Mode 3	31.6672	32.9096	33.3802	33.5501	33.5882
Mode 4	39.9765	41.5448	42.1389	42.3533	42.4014
Mode 5	42.4893	44.1561	44.7876	45.0155	45.0667
Mode 6	48.9610	53.0705	53.8294	54.1034	54.1648

parts. These parts are FG column, steel liquid storage tank and spring. FG column and springs are fixed to the floors as built-in. The liquid storage tank is made of standard steel and has a curb weight of 5000 kg and a fully loaded weight of 80000 kg. The first combination of FG column is made of aluminum as inner material and steel as outer material and second combination is made of aluminum as inner material and zirconia as outer material. Mechanical properties for zirconia, steel and aluminum materials are given in Table 1. The FG column is sized 40 m in length and 1.8 m in diameter (L=40 m, R=1.8 m). Various parameters have used to examine the vibration frequency within the scope of the mathematical procedure of the study. Functionally Graded index (β), empty, half full and completely full mass of storage tank parameters have conducted in following analyzes.

In the vibration analysis comparisons, firstly, the effect of the FG index (beta) parameter on the frequency parameter in the first six mode numbers of vibration was investigated. In this comparison, the FG index (β) value was changed between 0-4 values while other features remained constant, and the effects of this change on the vibration frequency were observed. The values obtained as a result of the calculations are presented in Tables 2 and 3.

The values presented in Tables 2 and Table 3 are visualized in Figs. 7, 8, 9 and 10 with different priority graphs, respectively. Among the graphs prepared for the same frequency parameter values, the graph lines in Fig. 5 belong to the mode numbers, while the graph lines in the Fig. 6 belong to the FG index values.

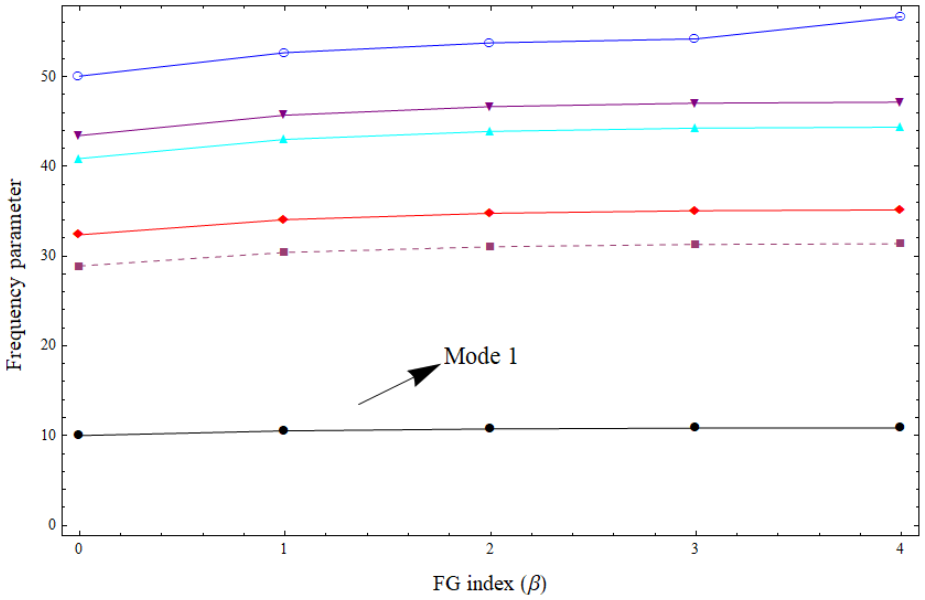

Fig. 7 Effects of FG (steel-aluminum) index on frequency for first six mode numbers

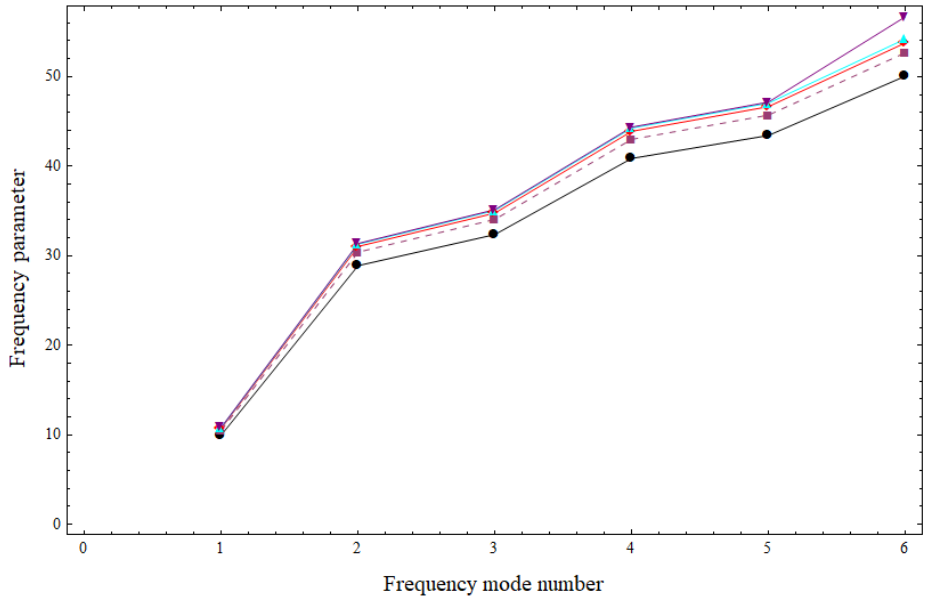

Fig. 8 Effects of FG (steel-aluminum) index on frequency for each six mode numbers for FG index

As can be seen in the tables and figures above, it has been observed that as the FG index value increases, the frequency parameter value also increases in all mode numbers. This increase is more clearly seen at higher mode numbers.

Another comparison related to the vibration frequency parameter was analyzed as mass changes. In this analysis, the cases where the liquid storage tank is completely empty (m=5000

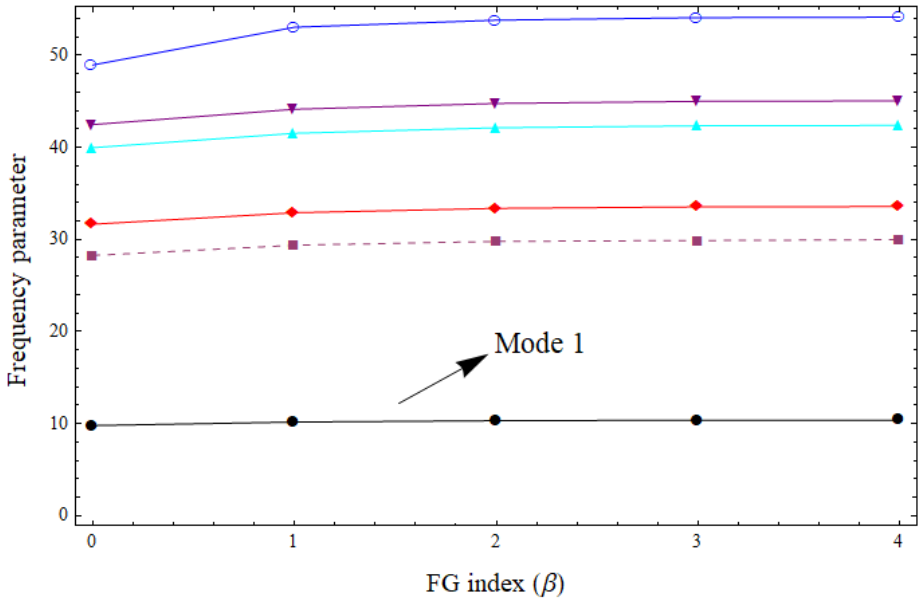

Fig. 9 Effects of FG (zirconia-aluminum) index on frequency for first six mode numbers

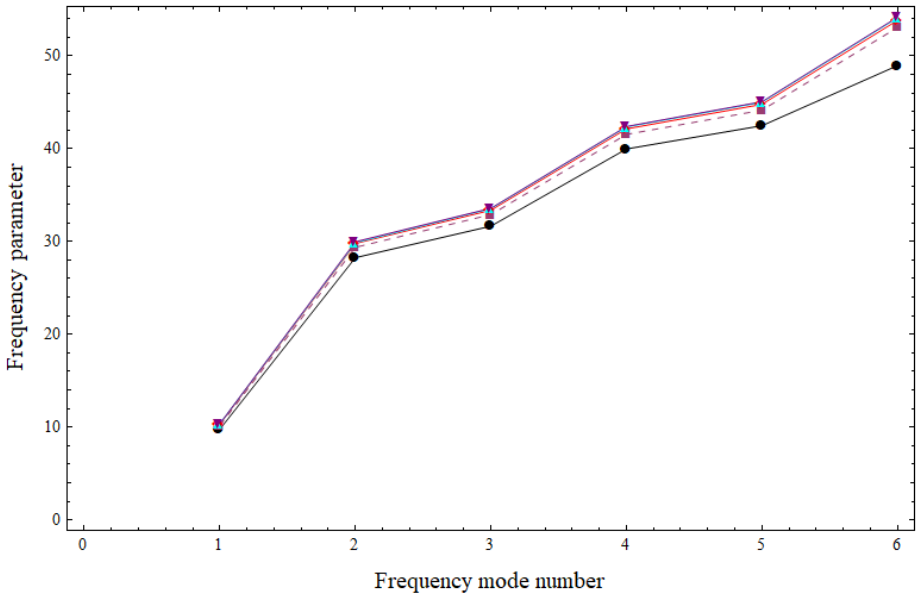

Fig. 10 Effects of FG (zirconia-aluminum) index on frequency for each six mode numbers for FG index

kg), approximately half full (m=40000 kg), finally completely full (m=80000 kg) and 2 other mass values were compared. The values of the vibration frequency parameter obtained as a result of these analyzes are given in Tables 4 and 5. In these calculations, the FG index value was taken as a constant zero ($\beta = 0$).

The frequency parameter values that change with the mass changes given in Tables 4 and 5 are

Table 4 Frequency parameter values (rad/s) for different mass values (steel-aluminum)

	m=5000 kg	*m*=15000 kg	*m*=25000 kg	*m*=40000 kg	*m*=80000 kg
Mode 1	14.1433	12.3285	11.5659	10.9060	10.0090
Mode 2	28.8989	28.8989	28.8989	28.8989	28.8989
Mode 3	32.3745	32.3745	32.3745	32.3745	32.3745
Mode 4	40.8692	40.8692	40.8692	40.8692	40.8692
Mode 5	43.4381	43.4381	43.4381	43.4381	43.4381
Mode 6	50.0543	50.0543	50.0543	50.0543	50.0543

Table 5 Frequency parameter values (rad/s) for different mass values (zirconia-aluminum)

	m=5000 kg	*m*=15000 kg	*m*=25000 kg	*m*=40000 kg	*m*=80000 kg
Mode 1	13.8343	12.0592	11.3133	10.6678	9.7824
Mode 2	28.2676	28.2676	28.2676	28.2676	28.2676
Mode 3	31.6673	31.6673	31.6673	31.6673	31.6673
Mode 4	39.9765	39.9765	39.9765	39.9765	39.9765
Mode 5	42.4893	42.4893	42.4893	42.4893	42.4893
Mode 6	48.9610	48.9610	48.9610	48.9610	48.9610

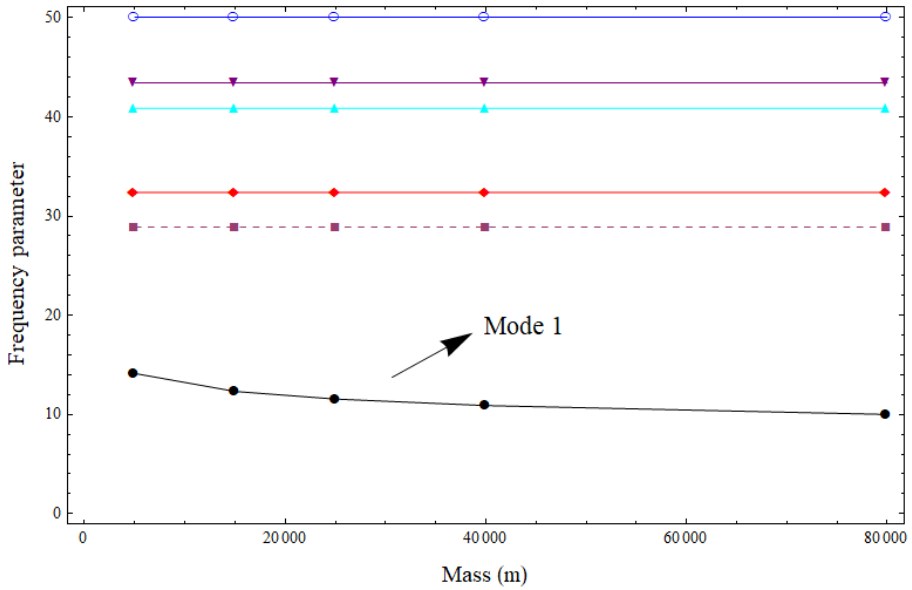

Fig. 11 Effects of mass on frequency for first six mode numbers (steel-aluminum)

graphed in Figs. 11, 12, 13 and 14 to see the changes more easily. In Figs. 11 and 13, the frequency parameter changes in the first six mode numbers as a result of mass changes are shown specifically for mode numbers. In Figs. 12 and 14, the values used for the same changes are presented in particular for mass changes this time.

As seen in the tables and figures, it was determined that the frequency parameter value decreased as the mass increased for the first mode number. For the other mode numbers, it is seen that the mass change does not cause any change.

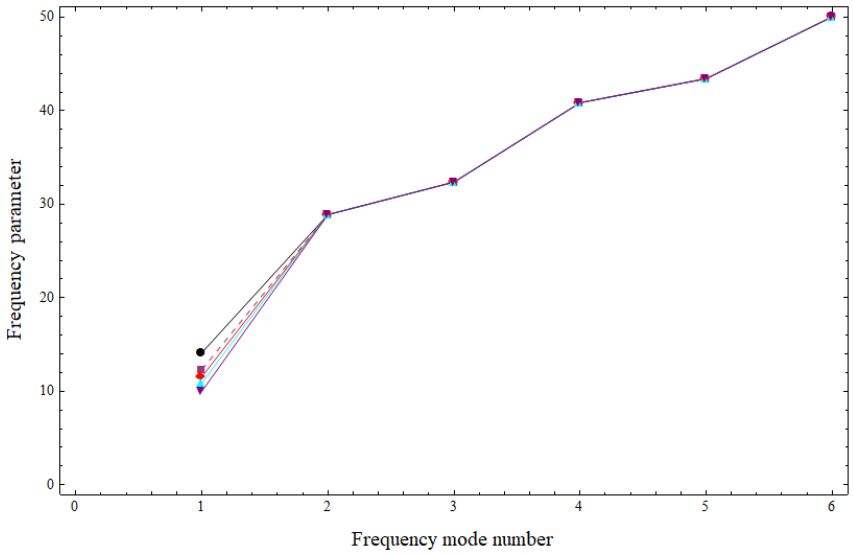

Fig. 12 Effects of mass on frequency for each six mode numbers for mass changes (steel-aluminum)

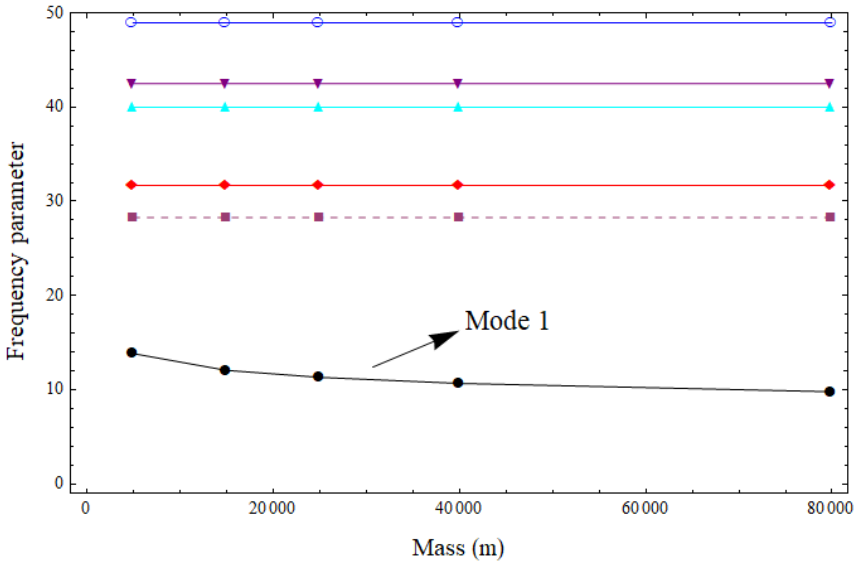

Fig. 13 Effects of mass on frequency for first six mode numbers (zircomia-aluminum)

The first six mode frequency parameter values obtained for the varying length values are given in Tables 6 and 7 and the graphically visualized versions of these values in Figs. 15 and 16 are given.

5. Conclusions

In the analyzes made within the scope of this study, some specific parameters affecting the

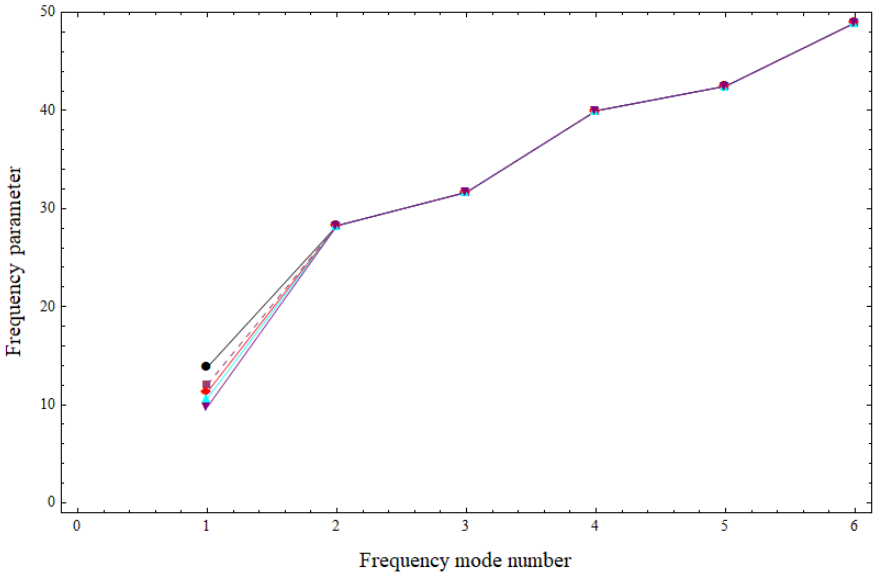

Fig. 14 Effects of mass on frequency for each six mode numbers for mass changes (zirconia-aluminum)

Table 6 Frequency parameter values (rad/s) for varying different length values (steel-aluminum)

	L=40 m	L=60 m	L=80 m	L=100 m
1	10.0009	4.9184	2.9728	2.0117
2	28.8989	12.8439	7.2247	4.6238
3	32.3745	14.3886	8.0936	5.1799
4	40.8692	18.1641	10.2173	6.5391
5	43.4381	19.3058	10.8595	6.9501
6	50.0543	22.2464	12.5136	8.0087

Table 7 Frequency parameter values (rad/s) for varying different length values (zirconia-aluminum)

	L=40 m	L=60 m	L=80 m	L=100 m
1	9.7824	4.8109	2.9078	1.9677
2	28.2676	14.0743	7.0669	5.0668
3	31.6672	18.8841	7.9168	6.7982
4	39.9765	21.7604	9.9941	8.1707
5	42.4893	22.6965	10.6223	9.3439
6	48.9610	25.9551	12.2402	10.1133

vibration frequency of a water tower modeled as a steel liquid storage tank fixed to a functionally graded column were investigated. These special parameters were chosen as β, which is the functional grading index, and m, which is the mass of the steel liquid storage tank. The change in the vibration frequency parameter as a result of the changes in these parameters has been presented in the previous section with tables and graphics.

1) As the beta value, which is the functional rating index, increases, the value of the vibration

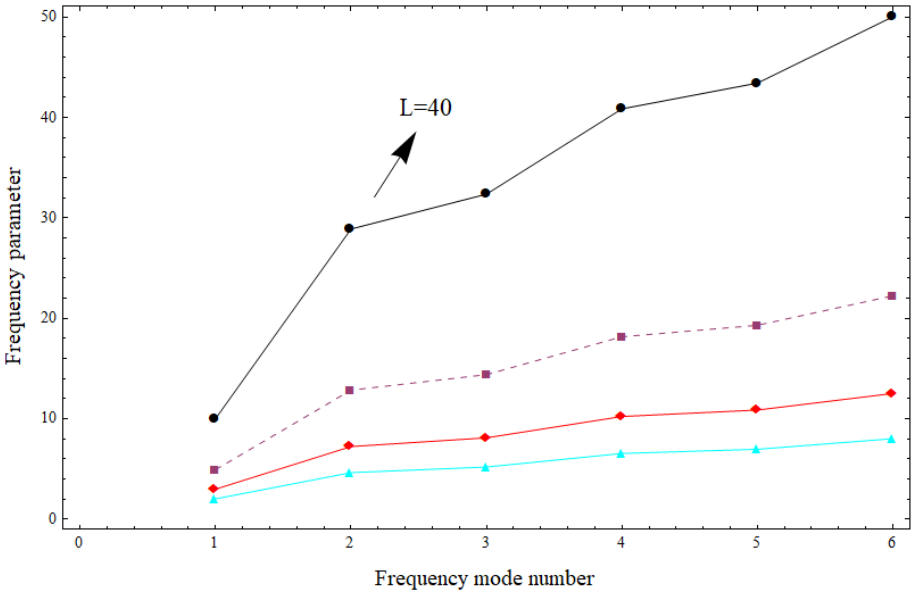

Fig. 15 Effects of column length on frequency for each six mode numbers for length changes (steel-aluminum)

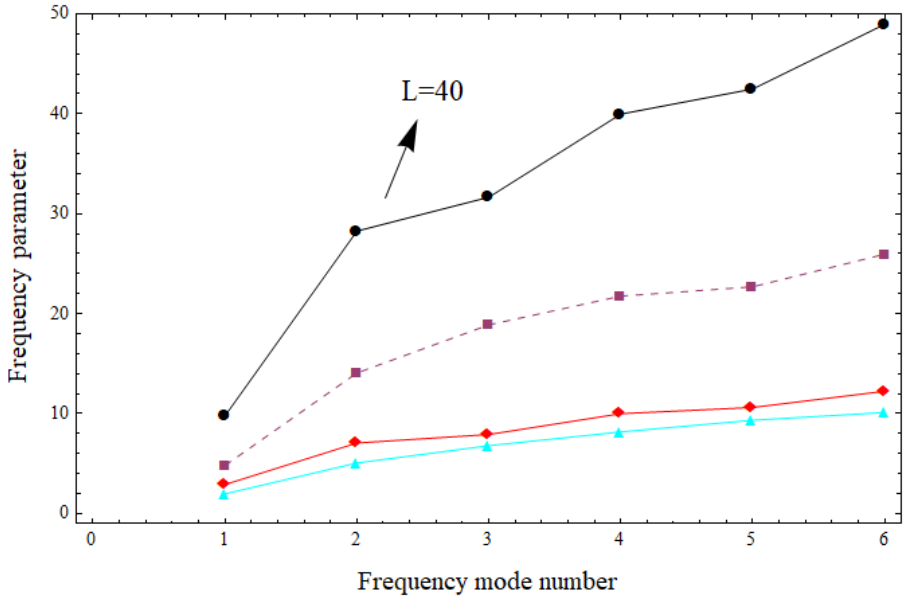

Fig. 16 Effects of column length on frequency for each six mode numbers for length changes (zirconia-aluminum)

frequency parameter also increases. While this increase is not obvious at lower mod numbers, it is clearly visible at higher mod numbers.

2) As the m value, which is the mass of the steel liquid storage tank, increases, it is seen that

there is a decrease in the vibration frequency parameter for the first mode number. However, mass changes in other mode numbers do not cause any change in the frequency parameter.

3) The frequency values of free vibration decrease as the L value increases, according to the mathematical operations with variable L values in the final part of this study.

4) Two different material combinations were selected in the analysis and calculations, and as a result of these calculations, similar graphics were observed in the two combinations. In other words, material changes do not affect the way the vibrations change, as seen in the analysis results.

References

Abdelrahman, A.A., Esen, I., Daikh, A.A. and Eltaher, M.A. (2021), "Dynamic analysis of FG nanobeam reinforced by carbon nanotubes and resting on elastic foundation under moving load", *Mech. Bas. Des. Struct. Mach.*, 1-24. https://doi.org/10.1080/15397734.2021.1999263.

Abdelrahman, A.A., Esen, I., Ozarpa, C., Shaltout, R., Eltaher, M.A. and Assie, A.E. (2021), "Dynamics of perforated higher order nanobeams subject to moving load using the nonlocal strain gradient theory", *Smart Struct. Syst*., **28**, 515-531. https://doi.org/10.12989/sss.2021.28.4.515.

Ali, B. and Dogangun, A. (2019), "Comparative investigation of dynamic analysis of cylindrical liquid storage tanks according to ACI 350 and EUROCODE 8", *Academic Platform Journal of Engineering and Science*, 7-3, 528-540.

Chen, C., Fung, C., Wang, H. and Chen, W. (2021), "Dynamic response of functionally graded carbon nanotube-reinforced hybrid composite plates", *J. Appl. Comput. Mech.*, https://doi.org/10.22055/jacm.2021.37884.3108.

Chen, J.Z. (2010), "Generalized SDOF system for dynamic analysis of concrete rectangular liquid storage tanks", Department of Civil Engineering Ryerson University.

Chen, J.Z. and Kianoush, M.R. (2009), "Generalized SDOF system for seismic analysis of concrete rectangular liquid storage tanks", *Eng. Struct.*, **31**, 2426-2435. https://doi.org/10.1016/j.engstruct.2009.05.019.

Chen, J.Z., Ghaemmaghami, A.R. and Kianoush, M.R. (2008), "Dynamic analysis of concrete rectangular liquid storage tanks", *The 14th World Conference on Earthquake Engineering*, Beijing, China, October.

Civalek, Ö., Uzun, B. and Yayli, M.Ö. (2021), "Longitudinal vibration analysis of FG nanorod restrained with axial springs using doublet mechanics", *Wave. Random Complex Media*, 1-23. https://doi.org/10.1080/17455030.2021.2000675.

Civalek, Ö., Uzun, B. and Yayli, M.Ö. (2022a), "Torsional vibrations of functionally graded restrained nanotubes", *Eur. Phys. J. Plus*, **137**, 113. https://doi.org/10.1140/epjp/s13360-021-02309-8.

Civalek, Ö., Uzun, B. and Yayli, M.Ö. (2022b), "Torsional and longitudinal vibration analysis of a porous nanorod with arbitrary boundaries", *Physica B: Condens. Matter.*, **633**, 413761. https://doi.org/10.1016/j.physb.2022.413761.

Daouadj, T.H. and Adim, B. (2017), "Mechanical behaviour of FGM sandwich plates using a quasi-3D higher order shear and normal deformation theory", *Struct. Eng. Mech.*, **61**(1), 49-63. https://doi.org/10.12989/sem.2017.61.1.049.

Doğangün, A. (1995), "Dikdörtgen kesitli su depolarının sonlu elemanlar yöntemiyle depo-sıvı-zemin etkileşimini dikkate alarak analitik yöntemlerle karşılaştırmalı deprem hesabı", Doctoral Dissertation, Karadeniz Technical University.

Esen, I., Abdelrahman, A.A. and Eltaher, M.A. (2021), "On vibration of sigmoid/symmetric functionally graded nonlocal strain gradient nanobeams under moving load", *Int. J. Mech. Mater. Des*., **17**, 721-742. https://doi.org/10.1007/s10999-021-09555-9.

Györgyi, J. (1981), "Frequency-dependent geometrical stiffness matrix for the vibration analysis of beam

systems", *Periodica Polytechnica Civil Eng.*, **25**(3-4), 151-163.
Györgyi, J. (1994), "Dynamic analysis of structures supporting a moving mass, exposed to external and internal damping", *Periodica Polytechnica Civil Eng.*, **38**(4), 387-398.
Haroun, M.A. (1980), "Dynamic analysis of liquid storage tanks", California Institute of Technology, Earthquake Engineering Research Laboratory.
Haroun, M.A. and Housner, G.W. (1981), "Earthquake response of deformable liquid storage tanks", *J. Appl. Mech.*, **48**, 411-418. https://doi.org/10.1115/1.3157631.
Jun, L., Dafu, X. and Bingyan, J. (2014), "Random structural dynamic response analysis under random excitation", *Periodica Polytechnica Civil Eng.*, **58**(3), 293-299. https://doi.org/10.3311/PPci.7523.
Kasimzade, A.A., Tuhta, S., Günday, F. and Aydın, H. (2021), "obtaining dynamic parameters by using ambient vibration recordings on model of the steel arch bridge", *Periodica Polytechnica Civil Eng.*, **65**(2), 608-618. https://doi.org/10.3311/PPci.16422.
Kotrosova, K. and Kormanikova, E. (2017), "Dynamic analysis of liquid storage tanks", *AIP Conf. Proc.*, **1863**, 260005. https://doi.org/10.1063/1.4992419.
Kozluca, G. and Nohutcu, H. (2007), "Betonarme silindirik su depolarinda ekonomik boyutlarin belirlenmesi", *J. Eng. Sci. Pamukkale Univ. Eng. Facult.*, **13**(3), 305-309.
Larkin, T. (2008), "Seismic response of liquid storage tanks incorporating soil structure interaction", *J. Geotech. Geoenviron. Eng.*, **134**(12), 1804-1814. https://doi.org/10.1061/(ASCE)1090-0241(2008)134:12(1804).
Malekzadeh Fard, K., Khajehdehi Kavanroodi, M., Malek-Mohammadi, H. and Pourmoayed, A. (2020), "Buckling and vibration analysis of a double-layer graphene sheet coupled with a piezoelectric nanoplate", *J. Appl. Comput. Mech.*, **8**(1), 129-143. https://doi.org/10.22055/jacm.2020.32145.1976.
Malhotra, P.K., Wenk, T. and Wieland, M. (2000), "Simple procedure for seismic analysis of liquid-storage tanks", *Struct. Eng. Int.*, **10**(3), 197-201. https://doi.org/10.2749/101686600780481509.
Nam Phan, H., Paolacci, F., Bursi, O.S. and Tondini, N. (2017), "Seismic fragility analysis of elevated steel storage tanks supported by reinforced concrete columns", *J. Loss Prev. Proc. Indus.*, **47**, 57-65. https://doi.org/10.1016/j.jlp.2017.02.017.
Németh, R.K. and Alzubaidi, B.M.A. (2021), "The effect of continuous suspension constraint on the free vibration and buckling of a beam", *Periodica Polytechnica Civil Eng.*, **65**(3), 977-987. https://doi.org/10.3311/PPci.17954.
Poloei, E., Zamanian, M. and Hosseini, S.A.A. (2017), "Nonlinear vibration analysis of an electrostatically excited micro cantilever beam coated by viscoelastic layer with the aim of finding the modified configuration", *Struct. Eng. Mech.*, **61**(2), 193-207. https://doi.org/10.12989/sem.2017.61.2.193.
Pourabdy, M., Shishesaz, M., Shahrooi, S. and Roknizadeh, S. (2021), "Analysis of axisymmetric vibration of functionally-graded circular nano-plate based on the integral form of the strain gradient model", *J. Appl. Comput. Mech.*, **7**(4), 2196-2220. https://doi.org/10.22055/jacm.2021.37461.3021.
Reddy, J.N. (2002), *Energy Principles and Variational Methods in Applied Mechanics*, Second Edition, John Wiley & Sons, New York.
Reddy, J.N. (2007), "Nonlocal theories for bending, buckling and vibration of beams", *Int. J. Eng. Sci*., **45**, 288-307. https://doi.org/10.1016/j.ijengsci.2007.04.004.
Rossit, C.A., Bambill, D.V. and Gilardi, G.J. (2017). "Free vibrations of AFG cantilever tapered beams carrying attached masses", *Struct. Eng. Mech.*, **61**(5), 685-691. https://doi.org/10.12989/sem.2017.61.5.685.
Ruiz, R.O., Lopez-Garcia, D. and Taflanidis, A.A. (2015), "An efficient computational procedure for the dynamic analysis of liquid storage tanks", *Eng. Struct.*, **85**, 206-218. https://doi.org/10.1016/j.engstruct.2014.12.011.
Sabuncu, O., Kacin, S., Gursoy, G. and Genes, M.C. (2013), "Mevcut bir su deposunun dinamik özelliklerinin titreşim kayitlari ile belirlenmesi", 2, Türkiye Deprem Mühendisliği ve Sismoloji Konferansı, Eylül, MKÜ, Hatay.
Soliman, A.E., Eltaher, M.A., Attia, M.A. and Alshorbagy, A.E. (2018), "Analysis of crack occurs under unsteady pressure and temperature in a natural gas facility by applying FGM", *Struct. Eng. Mech.*, **66**(1),

97-111. https://doi.org/10.12989/sem.2018.66.1.097.
Soliman, A.E., Eltaher, M.A., Attia, M.A. and Alshorbagy, A.E. (2018), "Nonlinear transient analysis of FG pipe subjected to internal pressure and unsteady temperature in a natural gas facility", *Struct. Eng. Mech.*, **66**(1), 85-96. https://doi.org/10.12989/sem.2018.66.1.085.
Tadi Beni, Z., Hosseini Ravandi, S. and Tadi Beni, Y. (2021), "Size-dependent nonlinear forced vibration analysis of Viscoelastic/Piezoelectric nano-beam", *J. Appl. Comput. Mech.*, **7**(4), 1878-1891. https://doi.org/10.22055/jacm.2020.32044.1958.
Veletsos, A.S. (1974), "Seismic effects in flexible liquid storage tanks", *Proceedings of the International Association for Earthquake Engineering Fifth World Conference*, Rome, June.
Vukobratovic, V. and Ladjinovic, D. (2013), "A simplified seismic analysis of circular liquid storage tanks", *Proceedings of the 6th PSU-UNS International Conference on Engineering and Technology (ICET-2013).*
Yayli, M.Ö. (2015), "Buckling analysis of a rotationally restrained single walled carbon nanotube", *Acta Physica Polonica A*, **127**, 3, 678-683. https://doi.org/10.24107/ijeas.252144.

CC